

Step-by-Step HHL Algorithm Walkthrough to Enhance the Understanding of Critical Quantum Computing Concepts

Hector Jose Morrell Jr and Hiu Yung Wong*

Department of Electrical Engineering,

San Jose State University, San Jose, CA 95192

(Dated: April 25, 2022)

Abstract

After learning basic quantum computing concepts, it is desirable to reinforce the learning using an important and relatively complex algorithm through which the students can observe and appreciate how the qubits evolve and interact with each other. Harrow-Hassidim-Lloyd (HHL) quantum algorithm, which can solve Linear System Problems with exponential speed-up over classical method and is the basic of many important quantum computing algorithms, is used to serve this purpose. The HHL algorithm is explained analytically followed by a 4-qubit numerical example in bra-ket notation. Matlab code corresponding to the numerical example is available for students to gain a deeper understanding of the HHL algorithm from a pure matrix point of view. A quantum circuit programmed using qiskit is also provided which can be used for real hardware execution in IBM quantum computers. After going through the material, students are expected to have a better appreciation of the concepts such as basis transformation, bra-ket and matrix representations, superposition, entanglement, controlled operations, measurement, Quantum Phase Estimation, Quantum Fourier Transformation, and quantum programming.

I. INTRODUCTION

Quantum Computing is promising in solving challenging engineering [1], biomedical [2] and finance [3] problems. It has a tremendous advancement in the last two decades and, recently, quantum supremacy has been demonstrated using a 53-qubit system [4]. Therefore, the training of a quantum technology workforce is an imminent goal for many countries (e.g. [5]) to support this fast-growing industry.

However, quantum technology is based on concepts very different from our daily and classical experience. In the early stage of learning quantum computing, although linking to daily and classical experience may enhance the understanding of certain quantum concepts and such an approach should not be de-emphasized, we believe a fast and robust way of training a quantum workforce is to train the students to be able to emulate a quantum processor and trace the evolution of the qubits. This is particularly useful in learning quantum algorithms without a quantum mechanics background. Such an approach obviates the students from cognitive conflicts, which can be resolved later, if possible, after they understand how

* hiuyung.wong@sjsu.edu

quantum computing works. This also embraces the “Shut up and calculate!” approach proposed by Mermin on how to deal with the uncomfortable feeling towards quantum mechanics interpretation [6].

Besides analytical equations, matrix representation and computer simulations are important tools to enhance the understanding of qubit evolution. However, available examples that include computer simulations are usually of simple algorithms and, very often, without matrix representation. There is a lack of examples of important and relatively complex algorithms which combine some of the most important quantum computing concepts and basic algorithms. Such examples are desirable to allow students to appreciate the roles and the interplay of various basic concepts in a more realistic quantum algorithm. Harrow-Hassidim-Lloyd (HHL) quantum algorithm [7][8] which can be used to solve linear system problems (LSP) and can provide exponential speedup over the classical conjugate gradient method is chosen for this purpose. HHL is the basic of many more advanced algorithms and is important in various applications such as machine learning [9] and modeling of quantum systems [2][10]. It has also been proposed to solve the Poisson equation [11][12]. In this paper, we detail the qubit evolution in Harrow-Hassidim-Lloyd (HHL) quantum algorithm analytically with a 4-qubit circuit as a numerical example. Although HHL examples are available (e.g. [13][14]), this paper has certain characteristics which are not all found in those examples. Firstly, the HHL algorithm is discussed analytically step-by-step and is self-contained. Secondly, a numerical example is given in bra-ket notation mirroring the analytical equations. Thirdly, a Matlab code corresponding exactly to the numerical example is available to enhance the understanding from a matrix point of view. The Matlab code allows the students to trace how the wavefunction evolves instead of just seeing the magnitude of the coefficients as in IBM-Q. Fourthly, a qiskit code written in python [15] corresponding to the numerical example is available and can be run in IBM simulation and hardware machines [16]. Finally, in the example, all the 4 qubits are traced throughout the process without simplification.

The readers are assumed to have the following background concepts which are further enhanced through the step-by-step walkthrough of the HHL algorithm: basis transformation, bra-ket and matrix representations, superposition, entanglement, encoding, controlled operations, measurement, Quantum Fourier Transformation, and quantum programming.

II. HHL ALGORITHM

A. Definitions and Overview

A linear system problem (LSP) can be represented as the following

$$A\vec{x} = \vec{b} \quad (1)$$

where A is an $N_b \times N_b$ Hermitian matrix and \vec{x} and \vec{b} are N_b -dimensional vectors. For simplicity, it is assumed $N_b = 2^{n_b}$. A and \vec{b} are known and \vec{x} is the unknown to be solved, i.e.

$$\vec{x} = A^{-1}\vec{b} \quad (2)$$

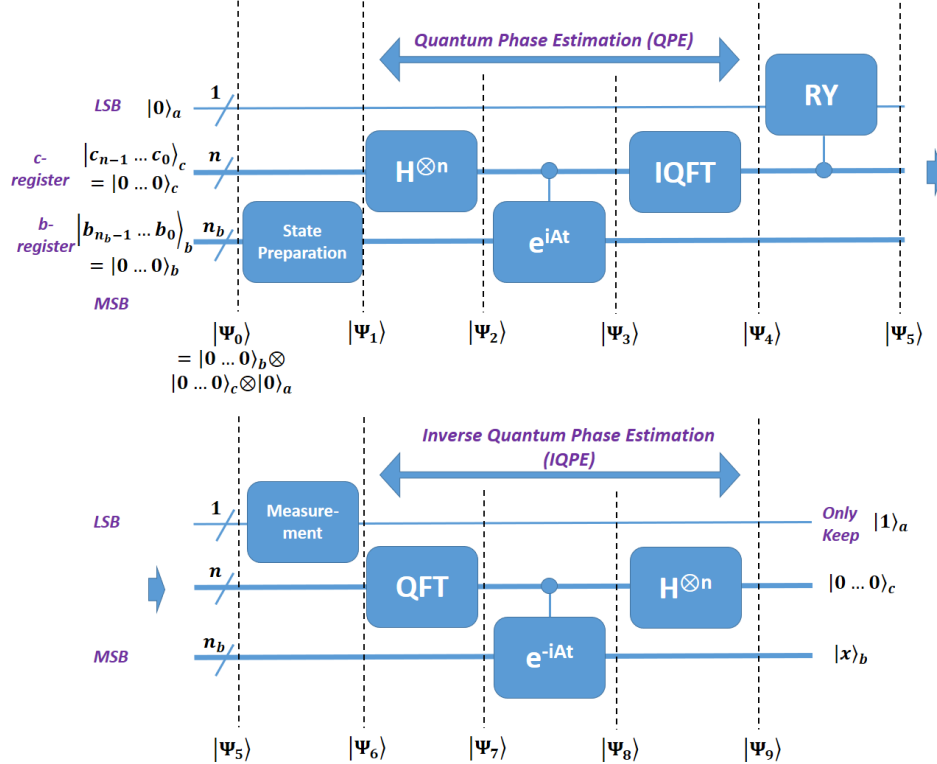


FIG. 1. Schematic of the HHL quantum circuit flowing from left to right. The circuit is decomposed into the top and bottom portions for clarity. Note that the lowest qubit in the diagram is the most significant bit (MSB) while the most top one is the least significant bit (LSB) by following the little-endian convention.

Figure 1 shows the schematic of the HHL algorithm and the corresponding circuit. In the HHL quantum algorithm, the N_b components of \vec{b} and \vec{x} are encoded as the amplitudes (*amplitude encoding*) of n_b -qubits, $| \rangle_b$, which form a \mathbb{C}^{N_b} Hibert space. n_b is chosen to be large enough to encode \vec{b} . These n_b -qubits are called b-register. The matrix A is simulated through *Hamiltonian encoding*. The HHL algorithm has 5 main components, namely state preparation, quantum phase estimation (QPE), ancilla bit rotation, inverse quantum phase estimation (IQPE), and measurement. In this paper, the little-endian convention is used in which the lowest qubit represents the most significant bit (MSB) and the most top qubit represents the least significant bit (LSB), which is a convention used in qiskit [15] and the IBM-Q platform [16]. Besides the n_b qubits for encoding the amplitudes in \vec{b} and eventually the result (the amplitudes in \vec{x}), an ancilla qubit $| \rangle_a$ and n other qubits $| \rangle_c$ (called clock qubits) are also required. The ancilla qubit, as its name implies, is important to help achieve the goal although it will be discarded at the end, as will be detailed later. The clock qubits are used to store the encoded eigenvalues of A and larger n results in higher accuracy when the encoding is not exact. The n clock qubits are also called c-register in this paper. We set $N = 2^n$.

The matrix A , which is a Hamiltonian, may be written as a linear combination of its eigenvectors, $|u_i\rangle$ weighted by its eigenvalues, λ_i .

$$A = \sum_{i=0}^{2^{n_b}-1} \lambda_i |u_i\rangle \langle u_i| \quad (3)$$

Since A is diagonal in its eigenvector basis, its inverse is simply, $A^{-1} = \sum_{i=0}^{2^{n_b}-1} \lambda_i^{-1} |u_i\rangle \langle u_i|$. \vec{b} can be also expressed in the basis of A , such that

$$|b\rangle = \sum_{j=0}^{2^{n_b}-1} b_j |u_j\rangle \quad (4)$$

Therefore, Eq. (2) can be encoded as,

$$|x\rangle = A^{-1} |b\rangle = \sum_{i=0}^{2^{n_b}-1} \lambda_i^{-1} b_i |u_i\rangle \quad (5)$$

by using the fact that $\langle u_i | u_j \rangle = \delta_{ij}$. The goal of the HHL algorithm is to find the solution in this form and $|x\rangle$ is stored in the b-register.

B. State Preparation

There are total $n_b + n + 1$ qubits and they are initialized as

$$|\Psi_0\rangle = |0 \cdots 0\rangle_b |0 \cdots 0\rangle_c |0\rangle_a = |0\rangle^{\otimes n_b} |0\rangle^{\otimes n} |0\rangle \quad (6)$$

In the state preparation, $|0 \cdots 0\rangle_b$ in the b-register needs to be rotated to have the amplitudes correspond to the coefficients of \vec{b} . That is

$$\vec{b} = \begin{pmatrix} \beta_0 \\ \beta_1 \\ \vdots \\ \beta_{N_b-1} \end{pmatrix} \Leftrightarrow \beta_0 |0\rangle + \beta_1 |1\rangle + \cdots + \beta_{N_b-1} |N_b-1\rangle = |b\rangle \quad (7)$$

The vector \vec{b} is represented in a column form on the left with coefficients β 's which is also a valid representation of $|b\rangle$. On the right, the corresponding basis of the Hilbert space formed by the n_b qubits is written explicitly. Therefore,

$$|\Phi_1\rangle = |b\rangle_b |0 \cdots 0\rangle_c |0\rangle_a \quad (8)$$

From now on, some of the subscripts of the kets will be omitted when there is no ambiguity. Since the state preparation depends on the actual value of \vec{b} , it will be discussed in more detail in the numerical example.

C. Quantum Phase Estimation

Quantum phase estimation (QPE) is also an eigenvalue estimation algorithm. QPE has three components, namely the superposition of the clock qubits through Hadamard gates, controlled rotation, and Inverse Quantum Fourier Transform (IQFT). Here we assume the readers are already familiar with IQFT and it will not be explained in detail. In the first step where a *superposition* of the clock qubits is created, Hadamard gates are applied to the clock qubits to obtain,

$$|\Psi_2\rangle = I^{\otimes n_b} \otimes H^{\otimes n} \otimes I |\Psi_1\rangle \quad (9)$$

$$= |b\rangle \frac{1}{2^{\frac{n}{2}}} (|0\rangle + |1\rangle)^{\otimes n} |0\rangle \quad (10)$$

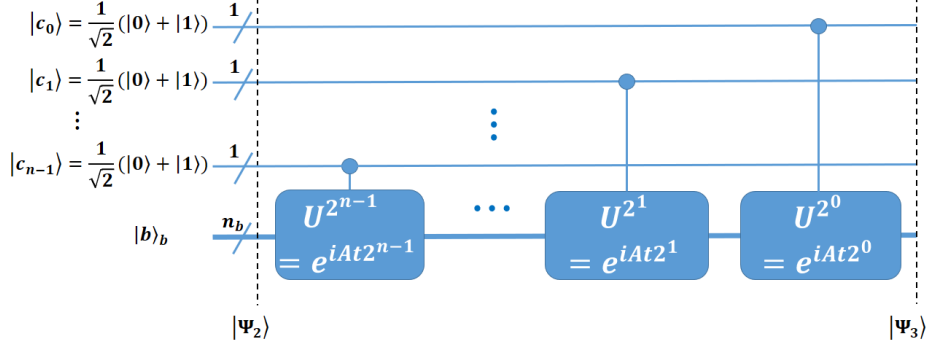


FIG. 2. The controlled-Rotation part of QPE. U is replaced by e^{iAt} in the HHL algorithm.

In the controlled rotation part, U is applied to $|b\rangle$ with the clock qubits as the control qubits (Figure 2). For simplicity, we begin by assuming that $|b\rangle$ is an eigenvector of U with eigenvalue $e^{2\pi i\phi}$. Therefore

$$U|b\rangle = e^{2\pi i\phi}|b\rangle \quad (11)$$

When the control clock qubit is $|0\rangle$, $|b\rangle$ will not be affected. If the clock bit is $|1\rangle$, U will be applied to $|b\rangle$. This is equivalent to multiplying $e^{2\pi i\phi 2^i}$ in front of the $|1\rangle$ of the i -th clock qubit. Therefore, after the controlled- U operation, we have

$$\begin{aligned} |\Psi_3\rangle &= |b\rangle \otimes \left(\frac{1}{2^{\frac{n}{2}}} (|0\rangle + e^{2\pi i\phi 2^{n-1}}|1\rangle) \otimes (|0\rangle + e^{2\pi i\phi 2^{n-2}}|1\rangle) \otimes \cdots \otimes (|0\rangle + e^{2\pi i\phi 2^0}|1\rangle) \right) \otimes |0\rangle_a \\ &= |b\rangle \frac{1}{2^{\frac{n}{2}}} \sum_{k=0}^{2^n-1} e^{2\pi i\phi k} |k\rangle |0\rangle_a \end{aligned} \quad (12)$$

In the IQFT part, only the clock qubits are affected. Note that in certain literature, this is called Quantum Fourier Transform (QFT).

$$\begin{aligned} |\Psi_4\rangle &= |b\rangle IQFT \left(\frac{1}{2^{\frac{n}{2}}} \sum_{k=0}^{2^n-1} e^{2\pi i\phi k} |k\rangle \right) |0\rangle_a \\ &= |b\rangle \frac{1}{2^{\frac{n}{2}}} \sum_{k=0}^{2^n-1} e^{2\pi i\phi k} (IQFT|k\rangle) |0\rangle_a \\ &= |b\rangle \frac{1}{2^n} \sum_{k=0}^{2^n-1} e^{2\pi i\phi k} \left(\sum_{y=0}^{2^n-1} e^{-2\pi i y k / N} |y\rangle \right) |0\rangle_a \\ &= \frac{1}{2^n} |b\rangle \sum_{y=0}^{2^n-1} \sum_{k=0}^{2^n-1} e^{2\pi i k (\phi - y / N)} |y\rangle |0\rangle_a \end{aligned} \quad (13)$$

Due to *interference*, only for $|y\rangle$ satisfying the condition $\phi - y/N = 0$ will have a finite amplitude of $\sum_{k=0}^{2^n-1} e^0 = 2^n$. Otherwise, the amplitude is $\sum_{k=0}^{2^n-1} e^{2\pi ik(\phi-y/N)} = 0$ due to *destructive interference*. By ignoring the states with zero amplitude, we may rewrite $|\Psi_4\rangle$ as

$$|\Psi_4\rangle = |b\rangle |N\phi\rangle |0\rangle_a \quad (14)$$

Therefore, in QPE, the clock qubits are used to represent the phase information of U , which is ϕ , and the accuracy depends on the number of qubits, n .

In *Hamiltonian encoding*, U is related to A through

$$U = e^{iAt} \quad (15)$$

where t is the evolution time for that Hamiltonian. U is obviously also diagonal in A' s eigenvector, $|u_i\rangle$, basis. If $|b\rangle = |u_j\rangle$,

$$U |b\rangle = e^{i\lambda_j t} |u_j\rangle \quad (16)$$

By equating $i\lambda_j t$ to $2\pi i\phi$ in Eq. (11), we get $\phi = \lambda_j t/2\pi$ and Eq. (14) becomes

$$|\Psi_4\rangle = |u_j\rangle |N\lambda_j t/2\pi\rangle |0\rangle_a \quad (17)$$

Thus the eigenvalues of A have been encoded in the clock qubits (*basis encoding*). However, in general, $|b\rangle = \sum_{j=0}^{2^{n_b}-1} b_j |u_j\rangle$ (Eq. 4), by using *superposition*,

$$|\Psi_4\rangle = \sum_{j=0}^{2^{n_b}-1} b_j |u_j\rangle |N\lambda_j t/2\pi\rangle |0\rangle_a \quad (18)$$

λ_j are usually not integers. We will choose t so that $\tilde{\lambda}_j = N\lambda_j t/2\pi$ are integers. Therefore, the encoded values $\tilde{\lambda}_j$ can be different from λ_j . Ψ_4 can be rewritten as

$$|\Psi_4\rangle = \sum_{j=0}^{2^{n_b}-1} b_j |u_j\rangle |\tilde{\lambda}_j\rangle |0\rangle_a \quad (19)$$

D. Controlled Rotation and Measurement of the Ancilla Qubit

The next step is to rotate the ancilla qubit, $|0\rangle_a$, based on the encoded eigenvalues in the c-register, such that

$$|\Psi_5\rangle = \sum_{j=0}^{2^{n_b}-1} b_j |u_j\rangle |\tilde{\lambda}_j\rangle \left(\sqrt{1 - \frac{C^2}{\tilde{\lambda}_j^2}} |0\rangle_a + \frac{C}{\tilde{\lambda}_j} |1\rangle_a \right) \quad (20)$$

where C is a constant. When the ancilla qubit is measured, the ancilla qubit *wavefunction* will *collapse* to either $|0\rangle$ or $|1\rangle$. If it is $|0\rangle$, the result will be discarded and the computation will be repeated until the measurement is $|1\rangle$. Therefore, the final wavefunction of interest is

$$|\Psi_6\rangle = \frac{1}{\sqrt{\sum_{j=0}^{2^{n_b}-1} \left| \frac{b_j C}{\tilde{\lambda}_j} \right|^2}} \sum_{j=0}^{2^{n_b}-1} b_j |u_j\rangle |\tilde{\lambda}_j\rangle \frac{C}{\tilde{\lambda}_j} |1\rangle_a \quad (21)$$

where the prefactor is due to normalization after measurement. Since $\left| \frac{C}{\tilde{\lambda}_j} \right|^2$ is the probability of obtaining $|1\rangle$ when the ancilla bit is measured, C should be chosen to be as large as possible. Compared to Eq. (5), the result resembles the answer $|x\rangle$ that we are looking for. However, it is *entangled* with the clock qubits, $|\tilde{\lambda}_j\rangle$. This means that we cannot factorize the result into a tensor product of the c-register and b-register. Therefore, we need to uncompute the state to *unentangle* them.

The measurement can be and is usually performed after uncomputation. However, since the ancilla bit is not involved in any operations after the controlled rotation, measuring the ancilla bit before the uncomputation gives the same result. For simplicity in the derivation, it is thus performed before the uncomputation.

E. Uncomputation - Inverse QPE

Firstly, QFT is applied to the clock qubits.

$$\begin{aligned} |\Psi_7\rangle &= \frac{1}{\sqrt{\sum_{j=0}^{2^{n_b}-1} \left| \frac{b_j C}{\tilde{\lambda}_j} \right|^2}} \sum_{j=0}^{2^{n_b}-1} \frac{b_j C}{\tilde{\lambda}_j} |u_j\rangle QFT |\tilde{\lambda}_j\rangle |1\rangle_a \\ &= \frac{1}{\sqrt{\sum_{j=0}^{2^{n_b}-1} \left| \frac{b_j C}{\tilde{\lambda}_j} \right|^2}} \sum_{j=0}^{2^{n_b}-1} \frac{b_j C}{\tilde{\lambda}_j} |u_j\rangle \left(\frac{1}{2^{n/2}} \sum_{y=0}^{2^n-1} e^{2\pi i y \tilde{\lambda}_j / N} |y\rangle \right) |1\rangle_a \end{aligned} \quad (22)$$

Then inverse controlled-rotations of the b-register by the clock qubits are applied with $U^{-1} = e^{-iAt}$. Similar to the forward process, when the control clock qubit is $|0\rangle$, $|u_j\rangle$ will

not be affected. If the clock bit is $|1\rangle$, U^{-1} will be applied to $|u_j\rangle$. This is equivalent to multiplying $e^{-i\lambda_j t}$ in front of the $|1\rangle$ of the i -th clock bit. Therefore,

$$|\Psi_8\rangle = \frac{1}{2^{n/2} \sqrt{\sum_{j=0}^{2^{n_b}-1} \left| \frac{b_j C}{\tilde{\lambda}_j} \right|^2}} \sum_{j=0}^{2^{n_b}-1} \frac{b_j C}{\tilde{\lambda}_j} |u_j\rangle (e^{-i\lambda_j t y} \sum_{y=0}^{2^n-1} e^{2\pi i y \tilde{\lambda}_j / N} |y\rangle) |1\rangle_a \quad (23)$$

Since we have set $\tilde{\lambda}_j = N\lambda_j t / 2\pi$, therefore, the two exponential terms cancel each other and

$$\begin{aligned} |\Psi_8\rangle &= \frac{1}{2^{n/2} \sqrt{\sum_{j=0}^{2^{n_b}-1} \left| \frac{b_j C}{\tilde{\lambda}_j} \right|^2}} \sum_{j=0}^{2^{n_b}-1} \frac{b_j C}{\tilde{\lambda}_j} |u_j\rangle \sum_{y=0}^{2^n-1} |y\rangle |1\rangle_a \\ &= \frac{1}{2^{n/2} \frac{Nt}{2\pi} \sqrt{\sum_{j=0}^{2^{n_b}-1} \left| \frac{b_j C}{\tilde{\lambda}_j} \right|^2}} \sum_{j=0}^{2^{n_b}-1} \frac{b_j C}{\lambda_j} |u_j\rangle \sum_{y=0}^{2^n-1} |y\rangle |1\rangle_a \\ &= \frac{C}{2^{n/2} \sqrt{\sum_{j=0}^{2^{n_b}-1} \left| \frac{b_j C}{\lambda_j} \right|^2}} |x\rangle \sum_{y=0}^{2^n-1} |y\rangle |1\rangle_a \end{aligned} \quad (24)$$

The clock qubits and the b-register are now *unentangled* and the b-register stores $|x\rangle$. By applying the Hadamard gate on the clock qubits, finally, we have

$$\begin{aligned} |\Psi_9\rangle &= \frac{1}{\sqrt{\sum_{j=0}^{2^{n_b}-1} \left| \frac{b_j C}{\lambda_j} \right|^2}} \sum_{j=0}^{2^{n_b}-1} \frac{b_j C}{\lambda_j} |u_j\rangle |0\rangle^{\otimes n} |1\rangle_a \\ &= \frac{1}{\sqrt{\sum_{j=0}^{2^{n_b}-1} \left| \frac{b_j C}{\lambda_j} \right|^2}} |x\rangle_b |0\rangle_c^{\otimes n} |1\rangle_a \end{aligned} \quad (25)$$

III. NUMERICAL EXAMPLE

We will present a numerical example and apply HHL to it step-by-step. Firstly, we will discuss how to implement the controlled- U and ancilla qubit rotations.

A. Encoding Scheme

In this example, the matrix A and vector \vec{b} are set to be

$$A = \begin{pmatrix} 1 & -\frac{1}{3} \\ -\frac{1}{3} & 1 \end{pmatrix} \quad (26)$$

$$\vec{b} = \begin{pmatrix} 0 \\ 1 \end{pmatrix} \quad (27)$$

The eigenvectors of A are $\vec{u}_0 = \begin{pmatrix} \frac{-1}{\sqrt{2}} \\ \frac{-1}{\sqrt{2}} \end{pmatrix}$, $\vec{u}_1 = \begin{pmatrix} \frac{-1}{\sqrt{2}} \\ \frac{1}{\sqrt{2}} \end{pmatrix}$ with eigenvalues $e_0 = \frac{2}{3}$ and $e_1 = \frac{4}{3}$ respectively. We need to use *basis encoding* to encode the eigenvalues in the basis formed by the clock qubit and 2 qubits are needed by encoding e_0 as $|01\rangle$ and e_1 as $|10\rangle$ so that it maintains the ratio of $e_1/e_0 = 2$. This means $\tilde{\lambda}_0 = 1$ and $\tilde{\lambda}_1 = 2$ or in other words, $|\tilde{\lambda}_0\rangle = |01\rangle$ and $|\tilde{\lambda}_1\rangle = |10\rangle$. This gives a perfect encoding with $n = 2$ (i.e. $N = 4$). Therefore, t is chosen to be $\frac{3\pi}{4}$ to achieve the encoding scheme since $\tilde{\lambda}_j = N\lambda_j t/2\pi$.

Since \vec{b} is a 2-dimensional complex vector, it can be encoded using 1 qubit and, thus, $n_b = 1$.

The solution to the LSP is found to be

$$\vec{x} = \begin{pmatrix} \frac{3}{8} \\ \frac{9}{8} \end{pmatrix} \quad (28)$$

whereby, the ratio of $|x_0|^2$ to $|x_1|^2$ is $1 : 9$.

B. $C - U$ Implementation

In reality, we expect the controlled- U operation to be implemented by a physical system with a Hamiltonian the same as the same as A . However, to understand the algorithm, we will derive the matrix for U and then map this to the $CU3$ gate used in IBM-Q. Since $n = 2$, there are two operations needed, namely $U^{2^1} = U^2$ and $U^{2^0} = U$, controlled by c_1 and c_0 , respectively.

In order to find the corresponding matrix for $U^2 = e^{i2At}$ and $U = e^{iAt}$, we need to perform *similarity transformation* on $i2At$ and iAt , exponentiate then, and transform back to the original basis.

The transformation matrix from the original basis to the eigenvector basis is

$$\begin{aligned} V &= \begin{pmatrix} \vec{u}_0 & \vec{u}_1 \end{pmatrix} \\ &= \begin{pmatrix} \frac{-1}{\sqrt{2}} & \frac{-1}{\sqrt{2}} \\ \frac{-1}{\sqrt{2}} & \frac{1}{\sqrt{2}} \end{pmatrix} \end{aligned} \quad (29)$$

Since V is real, its Hermitian conjugate, V^\dagger equals itself.

The diagonalized A , i.e. expressed in the basis formed by \vec{u}_0 and \vec{u}_1 , is

$$A_{diag} = \begin{pmatrix} \frac{2}{3} & 0 \\ 0 & \frac{4}{3} \end{pmatrix} \quad (30)$$

As it is diagonal, U can be obtained by exponentiating the elements accordingly.

$$\begin{aligned} U_{diag} &= \begin{pmatrix} e^{ie_0 t} & 0 \\ 0 & e^{ie_1 t} \end{pmatrix} \\ &= \begin{pmatrix} e^{i\pi/2} & 0 \\ 0 & e^{i\pi} \end{pmatrix} \\ &= \begin{pmatrix} i & 0 \\ 0 & -1 \end{pmatrix} \end{aligned} \quad (31)$$

and

$$U_{diag}^2 = \begin{pmatrix} -1 & 0 \\ 0 & 1 \end{pmatrix} \quad (32)$$

It is worth noting that both are naturally *unitary* which is a requirement for a quantum operation.

To obtain U and U^2 in the original basis, we only need to apply similarity transformation to them

$$\begin{aligned}
U &= VU_{diag}V^\dagger \\
&= \begin{pmatrix} \frac{-1}{\sqrt{2}} & \frac{-1}{\sqrt{2}} \\ \frac{-1}{\sqrt{2}} & \frac{1}{\sqrt{2}} \end{pmatrix} \begin{pmatrix} i & 0 \\ 0 & -1 \end{pmatrix} \begin{pmatrix} \frac{-1}{\sqrt{2}} & \frac{-1}{\sqrt{2}} \\ \frac{-1}{\sqrt{2}} & \frac{1}{\sqrt{2}} \end{pmatrix} \\
&= \frac{1}{2} \begin{pmatrix} -1+i & 1+i \\ 1+i & -1+i \end{pmatrix}
\end{aligned} \tag{33}$$

$$\begin{aligned}
U^2 &= VU_{diag}V^\dagger \\
&= \begin{pmatrix} \frac{-1}{\sqrt{2}} & \frac{-1}{\sqrt{2}} \\ \frac{-1}{\sqrt{2}} & \frac{1}{\sqrt{2}} \end{pmatrix} \begin{pmatrix} -1 & 0 \\ 0 & 1 \end{pmatrix} \begin{pmatrix} \frac{-1}{\sqrt{2}} & \frac{-1}{\sqrt{2}} \\ \frac{-1}{\sqrt{2}} & \frac{1}{\sqrt{2}} \end{pmatrix} \\
&= \begin{pmatrix} 0 & -1 \\ -1 & 0 \end{pmatrix}
\end{aligned} \tag{34}$$

$CU3$ -gate is chosen to implement U and U^2 , where

$$CU3 = \begin{pmatrix} e^{i\gamma} \cos(\theta/2) & -e^{i(\gamma+\lambda)} \sin(\theta/2) \\ e^{i(\gamma+\phi)} \sin(\theta/2) & e^{i(\gamma+\phi+\lambda)} \cos(\theta/2) \end{pmatrix} \tag{35}$$

By choosing $\theta = \pi, \phi = \pi, \lambda = 0, \gamma = 0$, U^2 is implemented.

By choosing $\theta = \pi/2, \phi = -\pi/2, \lambda = \pi/2, \gamma = 3\pi/4$, U is implemented.

Since in this example, $(U^2)^{-1} = U^2$, therefore, one can use the same set of parameters to implement $(U^2)^{-1}$.

However,

$$U^{-1} = \frac{1}{2} \begin{pmatrix} -1-i & 1-i \\ 1-i & -1-i \end{pmatrix} \tag{36}$$

We need to choose $\theta = \pi/2, \phi = \pi/2, \lambda = -\pi/2, \gamma = -3\pi/4$ to implement U^{-1} .

The controlled version of matrix U' can then be constructed using

$$C - U' = I \otimes |0\rangle\langle 0| + U' \otimes |1\rangle\langle 1| \tag{37}$$

Note that in this equation, only the controlling clock bit and the b-register are included for simplicity. For example,

$$\begin{aligned}
C - U^{-1} &= \begin{pmatrix} 1 & 0 \\ 0 & 1 \end{pmatrix} \otimes \begin{pmatrix} 1 & 0 \\ 0 & 0 \end{pmatrix} + \frac{1}{2} \begin{pmatrix} -1-i & 1-i \\ 1-i & -1-i \end{pmatrix} \otimes \begin{pmatrix} 0 & 0 \\ 0 & 1 \end{pmatrix} \\
&= \begin{pmatrix} 1 & 0 & 0 & 0 \\ 0 & 0 & 0 & 0 \\ 0 & 0 & 1 & 0 \\ 0 & 0 & 0 & 0 \end{pmatrix} + \frac{1}{2} \begin{pmatrix} 0 & 0 & 0 & 0 \\ 0 & -1-i & 0 & 1-i \\ 0 & 0 & 0 & 0 \\ 0 & 1-i & 0 & -1-i \end{pmatrix} \\
&= \frac{1}{2} \begin{pmatrix} 2 & 0 & 0 & 0 \\ 0 & -1-i & 0 & 1-i \\ 0 & 0 & 2 & 0 \\ 0 & 1-i & 0 & -1-i \end{pmatrix}
\end{aligned} \tag{38}$$

C. Implementataion of the Controlled-Rotation of Ancilla Qubit

The coefficients of $|0\rangle$ and $|1\rangle$ of the ancilla bit after rotation in Eq. (20) are $\sqrt{1 - \frac{C^2}{\tilde{\lambda}_j^2}}$ and $\frac{C}{\tilde{\lambda}_j}$, respectively. The sum of the square of the magnitudes of the coefficients is 1 as required. This means also $C \leq \tilde{\lambda}_j$. Since the minimal $\tilde{\lambda}_j$ is 1, we will set $C = 1$ to maximize the probability of measuring $|1\rangle$ during the ancilla bit measurement.

The transformation of $|0\rangle_a$ to $\sqrt{1 - \frac{1}{\tilde{\lambda}_j^2}} |0\rangle_a + \frac{1}{\tilde{\lambda}_j} |1\rangle_a$ is known to be equivalent to $RY(\theta)$ rotation,

$$RY(\theta) = \begin{pmatrix} \cos(\frac{\theta}{2}) & -\sin(\frac{\theta}{2}) \\ \sin(\frac{\theta}{2}) & \cos(\frac{\theta}{2}) \end{pmatrix} \tag{39}$$

with $\theta = 2 \arcsin(\frac{1}{\tilde{\lambda}_j})$. One can check this by multiplying $RY(\theta)$ to $|0\rangle_a$. Therefore, we will establish a function to implement this rotation and this function only need to be valid when the input are the encoded eigenvalues because only encoded eigenvalues have zero magnitudes in the c-register as shown in Eq. (19). The function is defined as

$$\theta(c) = \theta(c_1 c_0) = 2 \arcsin\left(\frac{1}{c}\right) \tag{40}$$

where c is the value of the clock qubits and c_1c_0 is its binary form.

Since only $|\tilde{\lambda}_j\rangle$ has non-zero amplitude in Eq. (19), we only need to set up Eq. (40) such that it is correct for $|c\rangle=|01\rangle$ and $|10\rangle$, namely

$$\theta(1) = \theta(01) = 2 \arcsin\left(\frac{1}{1}\right) = \pi \quad (41)$$

$$\theta(2) = \theta(10) = 2 \arcsin\left(\frac{1}{2}\right) = \frac{\pi}{3} \quad (42)$$

The following function can achieve the goal,

$$\theta(c) = \theta(c_1c_0) = \frac{\pi}{3}c_1 + \pi c_0 \quad (43)$$

Therefore, the controlled rotation can be implemented as

$$|1\rangle\langle 1| \otimes I \otimes RY\left(\frac{\pi}{3}\right) + |0\rangle\langle 0| \otimes I \otimes I + I \otimes |1\rangle\langle 1| \otimes RY(\pi) + I \otimes |0\rangle\langle 0| \otimes I \quad (44)$$

where the operators operate on qubits $|c_1\rangle$, $|c_0\rangle$, and $|a\rangle$ from left to right, respectively.

D. Quantum Circuit

An HHL circuit for the numerical example is then built and shown in Figure 3. We will then walk through the circuit using numerical substitution.

E. Numerical Substitution

The algorithm begins with

$$|\Psi_0\rangle = |0\rangle_b \otimes |00\rangle_c \otimes |0\rangle_a = |0000\rangle \quad (45)$$

X-gate is then applied to convert $|0\rangle_b$ to $|1\rangle_b$ with

$$|\Psi_1\rangle = X \otimes I \otimes I |\Psi_0\rangle = |1000\rangle \quad (46)$$

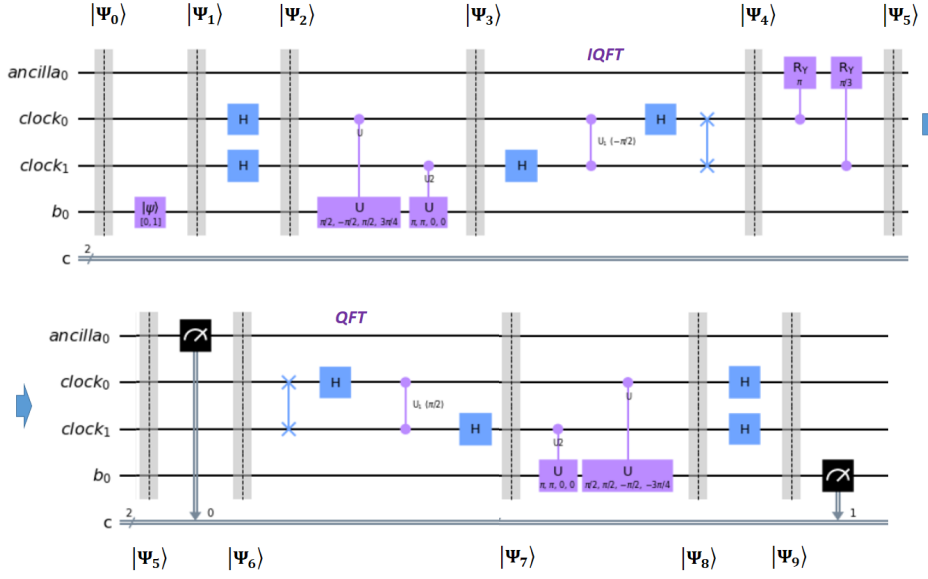


FIG. 3. The HHL circuit corresponding to the numerical example built to run in IBM-Q. This circuit is partitioned in the same way as the general HHL schematic in Figure 1.

After applying the Hadamard gates to create a superposition among the clock qubits,

$$\begin{aligned}
 |\Psi_2\rangle &= I \otimes H^{\otimes n} \otimes I |\Psi_1\rangle \\
 &= |1\rangle \frac{1}{2^{\frac{n}{2}}} (|0\rangle + |1\rangle)^{\otimes 2} |0\rangle \\
 &= \frac{1}{2} (|1000\rangle + |1010\rangle + |1100\rangle + |1110\rangle)
 \end{aligned} \tag{47}$$

Before applying the CU3 gates in the bra-ket notation, it will be convenient to perform a *basis change* to the eigenvector basis of A . Since $|1\rangle = \frac{1}{\sqrt{2}}(-|u_0\rangle + |u_1\rangle)$, we have $b_0 = \frac{-1}{\sqrt{2}}$ and $b_1 = \frac{1}{\sqrt{2}}$. Therefore,

$$\begin{aligned}
 |\Psi_2\rangle &= |1\rangle \frac{1}{2} (|000\rangle + |010\rangle + |100\rangle + |110\rangle) \\
 &= \frac{1}{\sqrt{2}} (-|u_0\rangle + |u_1\rangle) \frac{1}{2} (|000\rangle + |010\rangle + |100\rangle + |110\rangle) \\
 &= \frac{1}{2\sqrt{2}} (-|u_0000\rangle - |u_0010\rangle - |u_0100\rangle - |u_0110\rangle \\
 &\quad + |u_1000\rangle + |u_1010\rangle + |u_1100\rangle + |u_1110\rangle)
 \end{aligned} \tag{48}$$

In the controlled rotation operations, when the corresponding c-register is $|k\rangle_c$, a phase change of $\phi_j = k\lambda_j t/2\pi$ is added (i.e. multiplied by $e^{2\pi i \phi_j}$) for $|u_j\rangle$. Since $t = \frac{3\pi}{4}$, $\lambda_0 = \frac{2}{3}$

and $\lambda_1 = \frac{4}{3}$, we have

$$\begin{aligned}
|\Psi_3\rangle &= \frac{1}{2\sqrt{2}}(-|u_0000\rangle - e^{2\pi i\phi_0}|u_0010\rangle - e^{2\pi i2\phi_0}|u_0100\rangle - e^{2\pi i3\phi_0}|u_0110\rangle \\
&\quad + |u_1000\rangle + e^{2\pi i\phi_1}|u_1010\rangle + e^{2\pi i2\phi_1}|u_1100\rangle + e^{2\pi i3\phi_1}|u_1110\rangle) \\
&= \frac{1}{2\sqrt{2}}(-|u_0000\rangle - e^{i\lambda_0 t}|u_0010\rangle - e^{i2\lambda_0 t}|u_0100\rangle - e^{i3\lambda_0 t}|u_0110\rangle \\
&\quad + |u_1000\rangle + e^{i\lambda_1 t}|u_1010\rangle + e^{i2\lambda_1 t}|u_1100\rangle + e^{i3\lambda_1 t}|u_1110\rangle) \\
&= \frac{1}{2\sqrt{2}}(-|u_0000\rangle - e^{i\pi/2}|u_0010\rangle - e^{i\pi}|u_0100\rangle - e^{i3\pi/2}|u_0110\rangle \\
&\quad + |u_1000\rangle + e^{i\pi}|u_1010\rangle + e^{i2\pi}|u_1100\rangle + e^{i3\pi}|u_1110\rangle) \\
&= \frac{1}{2\sqrt{2}}(-|u_0000\rangle - i|u_0010\rangle + |u_0100\rangle + i|u_0110\rangle \\
&\quad + |u_1000\rangle - |u_1010\rangle + |u_1100\rangle - |u_1110\rangle)
\end{aligned} \tag{49}$$

Before applying IQFT, the terms are regrouped for simplicity.

$$\begin{aligned}
|\Psi_3\rangle &= \frac{1}{2\sqrt{2}}((-|u_0\rangle + |u_1\rangle)|00\rangle + (-i|u_0\rangle - |u_1\rangle)|01\rangle \\
&\quad + (|u_0\rangle + |u_1\rangle)|10\rangle + (i|u_0\rangle - |u_1\rangle)|11\rangle)|0\rangle
\end{aligned} \tag{50}$$

Now apply IQFT to the clock qubits, e.g.

$$IQFT|10\rangle = IQFT|2\rangle \tag{51}$$

$$\begin{aligned}
&= \frac{1}{2^{2/2}} \sum_{y=0}^{2^2-1} e^{-2\pi i 2y/4} |y\rangle \\
&= \frac{1}{2}(|0\rangle - |1\rangle + |2\rangle - |3\rangle) \\
&= \frac{1}{2}(|00\rangle - |01\rangle + |10\rangle - |11\rangle)
\end{aligned} \tag{52}$$

Similarly,

$$IQFT|00\rangle = \frac{1}{2}(|00\rangle + |01\rangle + |10\rangle + |11\rangle) \tag{53}$$

$$IQFT|01\rangle = \frac{1}{2}(|00\rangle - i|01\rangle - |10\rangle + i|11\rangle) \tag{54}$$

$$IQFT|11\rangle = \frac{1}{2}(|00\rangle + i|01\rangle - |10\rangle - i|11\rangle) \tag{55}$$

Therefore, applying IQFT to $|\Psi_3\rangle$ and substituting Eq. (51) to (55),

$$\begin{aligned}
|\Psi_4\rangle &= IQFT |\Psi_3\rangle \\
&= \frac{1}{4\sqrt{2}} \\
&\quad ((-|u_0\rangle + |u_1\rangle)(|00\rangle + |01\rangle + |10\rangle + |11\rangle) + \\
&\quad (-i|u_0\rangle - |u_1\rangle)(|00\rangle - i|01\rangle - |10\rangle + i|11\rangle) + \\
&\quad (|u_0\rangle + |u_1\rangle)(|00\rangle - |01\rangle + |10\rangle - |11\rangle) + \\
&\quad (i|u_0\rangle - |u_1\rangle)(|00\rangle + i|01\rangle - |10\rangle - i|11\rangle)) |0\rangle \\
&= \frac{1}{\sqrt{2}} (-|u_0\rangle |01\rangle + |u_1\rangle |10\rangle) |0\rangle
\end{aligned} \tag{56}$$

It can be seen that after IQFT, the eigenvalues are encoded in the clock qubits as $|01\rangle$ and $|11\rangle$ with non-zero amplitudes due *constructive interference*. $b_0 = \frac{-1}{\sqrt{2}}$ and $b_1 = \frac{1}{\sqrt{2}}$. We clearly see the entanglement between the b-register and the c-register that $|u_0\rangle$ goes with $|01\rangle$ and $|u_1\rangle$ goes with $|11\rangle$.

After performing the ancilla qubit rotation,

$$\begin{aligned}
|\Psi_5\rangle &= \sum_{j=0}^{2^1-1} b_j |u_j\rangle |\tilde{\lambda}_j\rangle \left(\sqrt{1 - \frac{C^2}{\tilde{\lambda}_j^2}} |0\rangle + \frac{C}{\tilde{\lambda}_j} |1\rangle \right) \\
&= -\frac{1}{\sqrt{2}} |u_0\rangle |01\rangle \left(\sqrt{1 - \frac{1}{1^2}} |0\rangle + \frac{1}{1} |1\rangle \right) + \\
&\quad \frac{1}{\sqrt{2}} |u_1\rangle |10\rangle \left(\sqrt{1 - \frac{1}{2^2}} |0\rangle + \frac{1}{2} |1\rangle \right)
\end{aligned} \tag{57}$$

If the measurement of the ancilla bit is $|1\rangle$,

$$|\Psi_6\rangle = \sqrt{\frac{8}{5}} \left(-\frac{1}{\sqrt{2}} |u_0\rangle |01\rangle |1\rangle + \frac{1}{2\sqrt{2}} |u_1\rangle |10\rangle |1\rangle \right) \tag{58}$$

Applying QFT to the encoded eigenvalues, we have

$$\begin{aligned}
QFT |10\rangle &= QFT |2\rangle \\
&= \frac{1}{2^{2/2}} \sum_{y=0}^{2^2-1} e^{2\pi i 2y/4} |y\rangle \\
&= \frac{1}{2} (|00\rangle - |01\rangle + |10\rangle - |11\rangle)
\end{aligned} \tag{59}$$

$$\begin{aligned}
QFT |01\rangle &= QFT |1\rangle \\
&= \frac{1}{2} (|00\rangle + i|01\rangle - |10\rangle - i|11\rangle)
\end{aligned} \tag{60}$$

Therefore, applying QFT to $|\Psi_6\rangle$ and substituting Eq. (59) to (60), we obtain

$$|\Psi_7\rangle = \sqrt{\frac{8}{5}} \left(-\frac{1}{\sqrt{2}} |u_0\rangle \frac{1}{2} (|00\rangle + i|01\rangle - |10\rangle - i|11\rangle) |1\rangle + \frac{1}{2\sqrt{2}} |u_1\rangle \frac{1}{2} (|00\rangle - |01\rangle + |10\rangle - |11\rangle) |1\rangle \right) |1\rangle \quad (61)$$

For the controlled rotation, the state is multiplied by $e^{-i\lambda_j t}$ and $e^{-i2\lambda_j t}$ if $c_0 = 1$ and $c_1 = 1$, respectively. Since $e^{-i\lambda_0 t} = -i$, $e^{-i2\lambda_0 t} = -1$, $e^{-i\lambda_1 t} = -1$, $e^{-i2\lambda_1 t} = 1$, and $Nt/2\pi = 3/2$

$$\begin{aligned} |\Psi_8\rangle &= \sqrt{\frac{8}{5}} \left(-\frac{1}{\sqrt{2}} |u_0\rangle \frac{1}{2} (|00\rangle + |01\rangle + |10\rangle + |11\rangle) |1\rangle + \frac{1}{2\sqrt{2}} |u_1\rangle \frac{1}{2} (|00\rangle + |01\rangle + |10\rangle + |11\rangle) |1\rangle \right) |1\rangle \\ &= \frac{1}{2} \sqrt{\frac{8}{5}} \left(-\frac{1}{\sqrt{2}} |u_0\rangle + \frac{1}{2\sqrt{2}} |u_1\rangle \right) (|00\rangle + |01\rangle + |10\rangle + |11\rangle) |1\rangle \\ &= \frac{1}{2} \left(\frac{2}{3} \right) \sqrt{\frac{8}{5}} \left(-\frac{1}{\frac{2}{3}\sqrt{2}} |u_0\rangle + \frac{1}{\frac{4}{3}\sqrt{2}} |u_1\rangle \right) (|00\rangle + |01\rangle + |10\rangle + |11\rangle) |1\rangle \end{aligned} \quad (62)$$

Finally, by applying Hardamard gate to the clock qubits,

$$|\Psi_9\rangle = \frac{2}{3} \sqrt{\frac{8}{5}} \left(-\frac{1}{\frac{2}{3}\sqrt{2}} |u_0\rangle + \frac{1}{\frac{4}{3}\sqrt{2}} |u_1\rangle \right) |00\rangle |1\rangle \quad (63)$$

It can be verified that $|\Psi_9\rangle$ is a normalized vector as it should be because every operation in the HHL circuit is unitary and preserves the norm.

Eq. (63) can be simplified by substituting $|u_0\rangle = \frac{-1}{\sqrt{2}} |0\rangle + \frac{-1}{\sqrt{2}} |1\rangle$ and $|u_1\rangle = \frac{-1}{\sqrt{2}} |0\rangle + \frac{1}{\sqrt{2}} |1\rangle$. We obtain,

$$|\Psi_9\rangle = \frac{1}{2} \sqrt{\frac{2}{5}} (|0\rangle + 3|1\rangle) |00\rangle |1\rangle \quad (64)$$

The probability ratio of obtaining $|0\rangle$ and $|1\rangle$ when b-register is measured is thus 1 : 9 as expected.

F. Simulation Results

Matlab code implementing the numerical example using matrix approach is created and available at [17]. In the Matlab code, measurement is not performed (i.e. not partial tracing of the matrix). Ψ_9 is found to be

$$\begin{pmatrix} -0.4330 \\ 0.2500 \\ 0.0000 \\ -0.0000 \\ 0.0000 \\ -0.0000 \\ 0.0000 \\ 0.0000 \\ 0.4330 \\ 0.7500 \\ -0.0000 \\ 0.0000 \\ -0.0000 \\ 0.0000 \\ -0.0000 \\ 0.0000 \end{pmatrix} \quad (65)$$

Since $|0\rangle_c$ are discarded during the measurement step, only $|0001\rangle$ and $|1001\rangle$ are left. Their amplitude ratio is $0.25^2 : 0.75^2 = 1 : 9$ as expected.

The circuit in Fig. 3 is also simulated in the IBM-Q system (code available at [17]). Since only the b-register and the ancilla qubit are measured, there are only four possible outputs as shown in Figure 4. Again, only $|1\rangle_a$ should be considered. The ratio of the measurement probability of $|0\rangle_b |1\rangle_a$ to $|1\rangle_b |1\rangle_a$ is $0.063^2 : 0.564^2 = 1 : 8.95$, which is close to the expected value.

On the other hand, due to the imperfection and noise in a real quantum computer, the hardware execution of the same circuit does not give satisfactory result (Figure 5). The ratio of the measurement probability of $|0\rangle_b |1\rangle_a$ to $|1\rangle_b |1\rangle_a$ is only $0.142^2 : 0.361^2 = 1 : 2.54$.

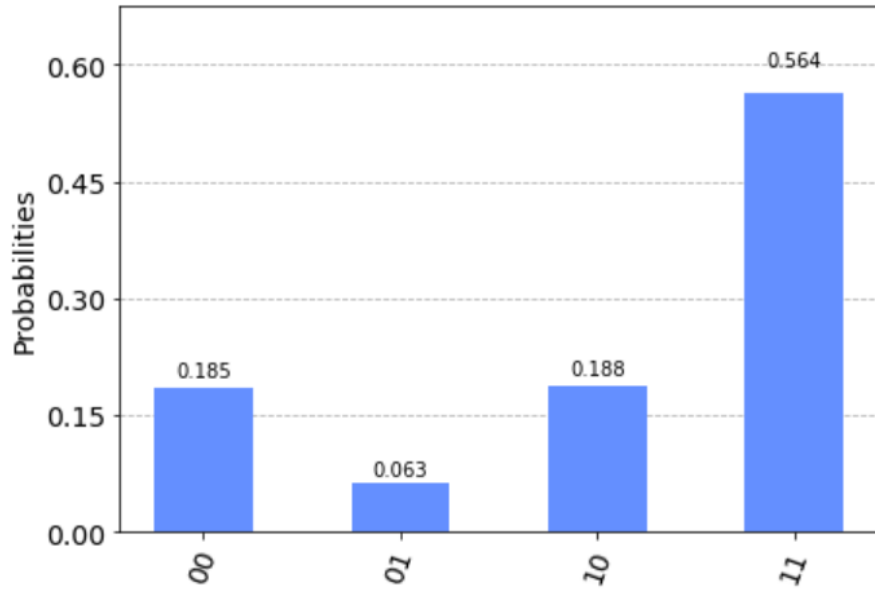


FIG. 4. Simulation result of the circuit in Figure 3 using IBM-Q. Only the MSB, $| \rangle_b$ and the LSB, $| \rangle_a$ are measured.

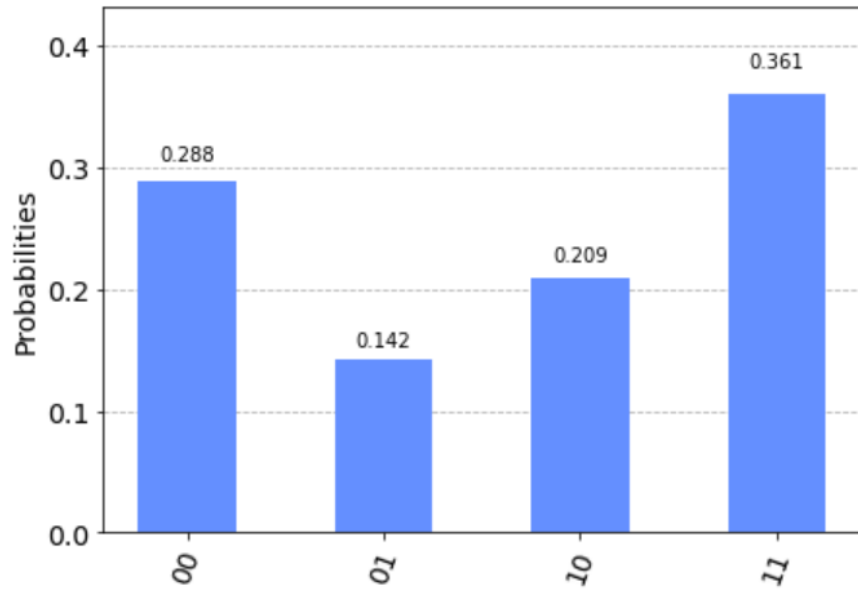


FIG. 5. Hardware result of the circuit in Figure 3 run in machine `ibmq_santiago`. Only the MSB, $| \rangle_b$ and the LSB, $| \rangle_a$ are measured.

IV. CONCLUSION

In this paper, we presented the HHL algorithm through a step-by-step walkthrough of the derivation. A numerical example is also presented in the bra-ket notation. The numerical example echos the analytical derivation to help students understand how qubits evolve in this important and relatively complex algorithm. A Matlab code corresponding to the numerical example is constructed to help understand the algorithm from the matrix point of view. Qiskit circuit of the corresponding circuit which can be simulated in IBM-Q and run on their quantum computing hardware is also available. Through this self-contained and step-by-step walkthrough, the basic concepts in quantum computing are reinforced.

- [1] P. W. Shor, “Algorithms for quantum computation: discrete logarithms and factoring,” Proceedings 35th Annual Symposium on Foundations of Computer Science, 1994, pp. 124–134, doi: 10.1109/SFCS.1994.365700.
- [2] C. Outeiral, M. Strahm, J. Shi, G. M. Morris, S. C. Benjamin, and C. M. Deane, “The prospects of quantum computing in computational molecular biology,” *WIREs Comput. Mol. Sci.*, **11**, e1481 (2021).
- [3] D. J. Egger et al., “Quantum Computing for Finance: State-of-the-Art and Future Prospects,” in *IEEE Transactions on Quantum Engineering*, **1**, pp. 1–24, 2020, Art no. 3101724, doi: 10.1109/TQE.2020.3030314.
- [4] F. Arute, K. Arya, R. Babbush et al., “Quantum supremacy using a programmable superconducting processor,” *Nature* **574**, 505–510 (2019). <https://doi.org/10.1038/s41586-019-1666-5>.
- [5] National Strategic Overview for Quantum Information Science Report (National Science and Technology Council, 2018). <https://www.whitehouse.gov/wp-content/uploads/2018/09/National-Strategic-Overview-for-Quantum-Information-Science.pdf>.
- [6] N. David Mermin, “Could Feynman Have Said This?,” *Physics Today* **57** (5), 10 (2004); doi: 10.1063/1.1768652
- [7] A. Harrow, A. Hassidim, and S. Lloyd, “Quantum algorithm for linear systems of equations,” *Phys. Rev. Lett.* **103**, 150502 (2009).

- [8] Yudong Cao, Anmer Daskin, Steven Frankel, and Sabre Kais, “Quantum circuit design for solving linear systems of equations,” *Molecular Physics* **110**, 15–16 (2011).
- [9] S. Dmitry et al., “The Potential of Quantum Computing and Machine Learning to Advance Clinical Research and Change the Practice of Medicine.” *Missouri medicine* **115** (5), 463–467 (2018).
- [10] Bojia Duan, Jiabin Yuan, Chao-Hua Yu, Jianbang Huang, and Chang-Yu Hsieh, “A survey on HHL algorithm: From theory to application in quantum machine learning”, *Physics Letters A* **384**, 126595 (2020).
- [11] Shengbin Wang, Zhimin Wang, Wendong Li, Lixin Fan, Zhiqiang Wei, and Yongjian Gu, “Quantum fast Poisson solver: the algorithm and complete and modular circuit design,” *Quantum Information Processing* **19**, Article number: 170 (2020).
- [12] Hector Morrell and Hiu Yung Wong, “Study of using Quantum Computer to Solve Poisson Equation in Gate Insulators,” *arXiv:2107.06378*.
- [13] Schleich, P., 2019. How to solve a linear system of equations using a quantum computer. http://www.acom.rwth-aachen.de/_media/3teaching/00projects/schleich.pdf.
- [14] HHL Example using Qiskit, <https://qiskit.org/textbook/ch-applications/hhl_tutorial.html>.
- [15] Gadi Aleksandrowicz, et al., (2019). Qiskit: An Open-source Framework for Quantum Computing (0.7.2). Zenodo. <https://doi.org/10.5281/zenodo.2562111>.
- [16] IBM Quantum Site, <<https://quantum-computing.ibm.com/>>.
- [17] Matlab code and Jupyter Notebook, <https://github.com/hywong2/HHL_Example>.